

Electronic Supplementary Information

Pd²⁺ fluorescent sensors based on amino and imino derivatives of rhodamine and improvement of water solubility by the formation of inclusion complexes with β -cyclodextrin

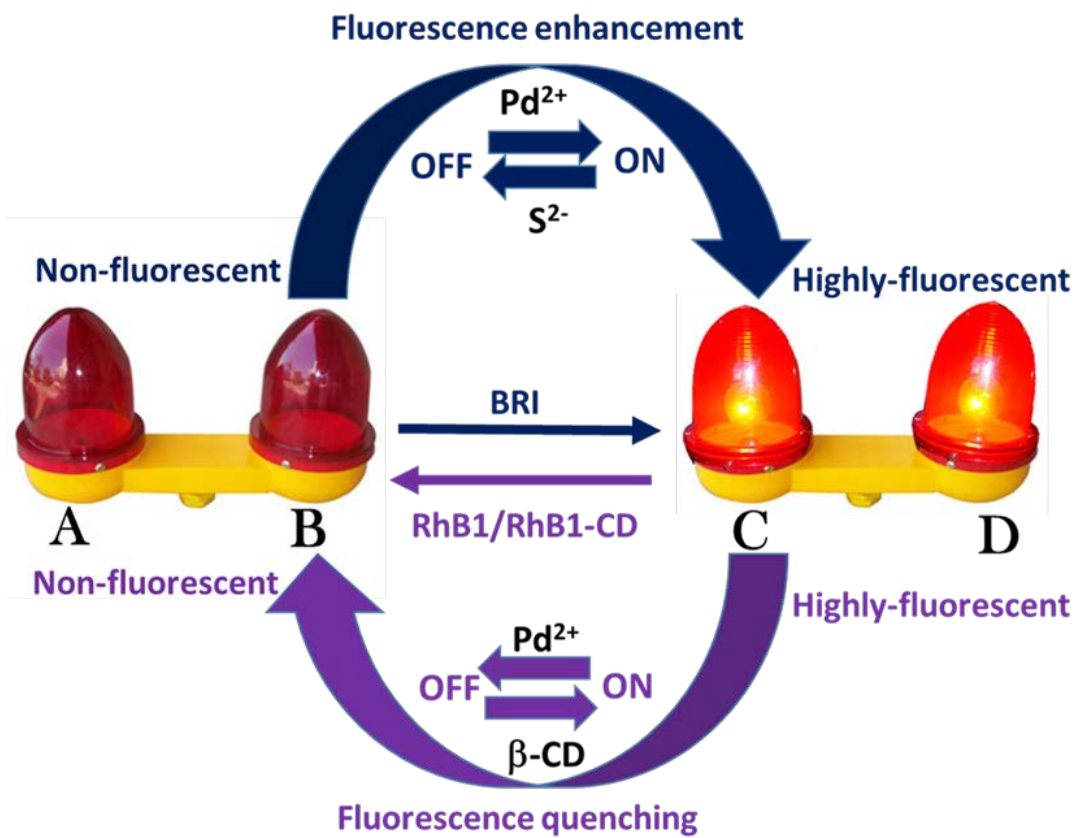
Yan-Song Zhang^a, Rathinam Balamurugan^a, Jian-Chin Lin^a, Sri Fitriyani^a, Jui Hsiang Liu^{a*} and Alexander Emelyanenko^b

Received (in XXX, XXX) XthXXXXXXXXXX 20XX, Accepted Xth XXXXXXXXXXXX 20XX
DOI: 10.1039/b000000x

Department of Chemical Engineering, National Cheng Kung University, Tainan 70101, Taiwan, Republic of China. Fax: +886-6- 2384590; Tel: +886-6-2757575ext.62646 E-mail: jhliu@mail.ncku.edu.tw

Contents	Page No.
1. Graphical Figure	S3
2. Synthesis of rhodamine B hydrazide and bis-rhodamine imine (BRI)	S4
3. Synthesis of RhB1	S5
4. Synthesis of RhB1-cyclodextrin inclusion complexes	S6
5. Fig. S1 Infrared spectrum of rhodamine B hydrazide	S7
6. Fig. S2 Infrared spectrum of BRI probe	S8
7. Fig. S3 ¹ H-NMR spectrum of rhodamine B hydrazide in CDCl ₃	S9
8. Fig. S4 ¹ H-NMR spectrum of probe BRI in CDCl ₃ .	S10
9. Fig. S5 ¹³ C-NMR spectrum of probe BRI in CDCl ₃	S11
10. Fig. S6 DEPT135 ¹³ C-NMR spectrum of probe BRI in CDCl ₃	S12
11. Fig. S7 Elemental analysis of BRI	S13
12. Fig. S8 Mass spectrometric analysis of BRI	S14
13. Fig. S9 ¹ H-NMR spectrum of RhB1-CD in D ₂ O	S15
14. Fig. S10 2D- ¹ H-NMR spectrum of RhB1-CD in D ₂ O	S16
15. Fig. S11 2D- ¹ H-NMR spectrum of RhB1-CD in D ₂ O	S17
16. Fig. S12 Comparison of the ¹ H-NMR signal of RhB1 and RhB1-CD between 1.1~1.2 ppm	S18
17. Fig. S13 Comparison of the ¹ H-NMR signal of RhB1 and RhB1-CD between 6.2 and 6.5 ppm	S18
18. Fig. S14 Mass spectrum of RhB1-CD	S19
19. Fig. S15 Mass spectrum of RhB1- RhB1	S19
20. Fig. S16 Real images of BRI (10 μ M) in CH ₃ CN:H ₂ O (3:2 v/v)	

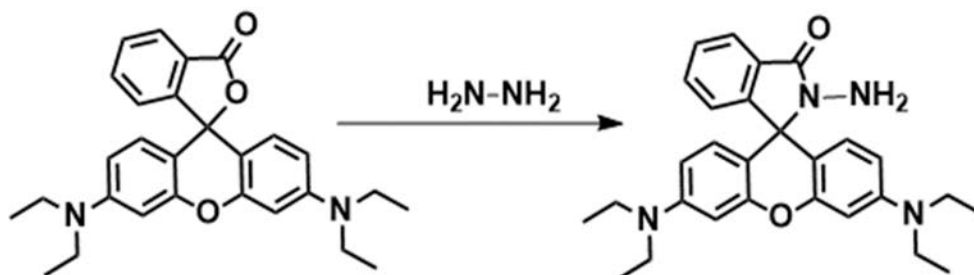
in the presence of metal ions (1 mM, 100 equivalents) under visible light (top) and UV lamp (bottom).	S20
21. Fig. S17. (a) Fluorescence spectral changes of BRI (10 μ M) upon addition of 100 equivalents of metal ions. (b) Normalized fluorescence spectra of BRI (10 μ M) in CH ₃ CN:H ₂ O (3:2 v/v) in the presence of metal ions (1 mM, 100 equivalents), $\lambda_{\text{ex}}= 510$ nm.	S21
22. Fig. S18 (a) Time-dependent UV-vis spectra of BRI (10 μ M) with 100 equivalents of Pd ²⁺ in CH ₃ CN:H ₂ O (3:2 v/v). (b) Plot of absorbance of BRI/Pd ²⁺ at 555 nm as a function of time.	S22
23. Fig. S19 (a) UV-vis spectra of BRI (10 μ M) in CH ₃ CN:H ₂ O (3:2 v/v) solution containing various amounts of Pd ²⁺ ion (0.0-3.0 equivalents), $\lambda_{\text{max}}= 555$ nm. (b) Plot of the absorbance of BRI versus the amounts of Pd ²⁺ (0.0-3.0 equiv.) at $\lambda=555$ nm.	S23
24. Fig. S20 The Job plot for BRI-Pd ²⁺ showed 1:2 complexes	S24
25. Fig. S21 Hill plot of fluorescence probe BRI with Pd ²⁺	S25
26. Fig. S22 (a) Effect of pH on the absorbance of BRI (10 μ M) at 555 nm in CH ₃ CN:H ₂ O (3:2 v/v), where pH was adjusted using HCl (0.01 M). (b) Effect of pH on the structure of BRI	S26
27. Fig. S23 Interaction of various metal ions with RBI	S27
28. Fig. S24 Time-dependent UV-vis spectra of RhB1-CD (1 mM) with 100 equivalents of Pd ²⁺ in H ₂ O	S28
29. Fig. S25 Dependence of quenching ratio of RhB1-CD on Pd ²⁺ concentration	S29
30. Fig. S26. Binding mechanism of RhB1 with Pd ²⁺ in EtOH:H ₂ O (1:1)	S30
31. Fig. S27. Dependence of (a) UV-vis and (b) PL spectra of RhB1-CD on Pd ²⁺ concentration in H ₂ O at pH 7.0.	S31
32. Fig. S28 Titration of BRI-Pd ²⁺ complexes with Na ₂ S measured with (a) UV-vis and (b) fluorescence spectroscopy	S32
33. Fig. S29 Reversibility of BRI process in the presence of Na ₂ S	S33
34. Fig. S30. Fluorescence images of BRI (a and b) and BRI-Pd ²⁺ (c and d) under confocal laser scanning microscopy respectively	S34



BRI system: A to D = Rhodamine unit
 RhB1/RhB1-CD system: A & C = Rhodamine; B & D = free amino/β-CD

Graphical picture for BRI, RhB1-CD and their response with Pd²⁺

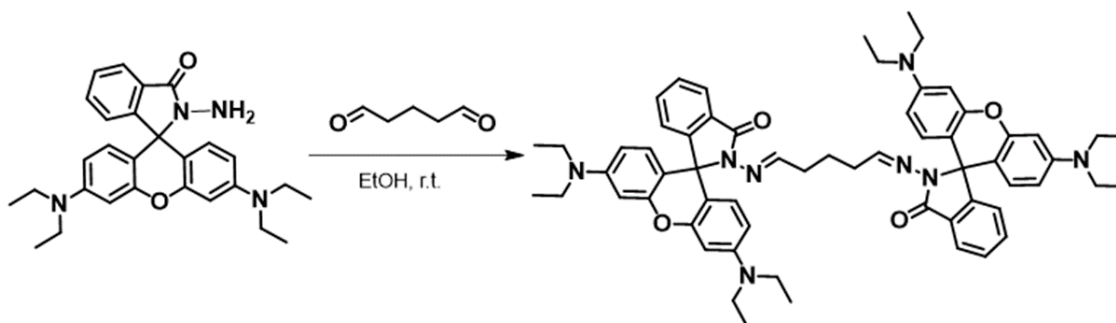
Synthesis of Rhodamine B Hydrazide (1)



Compound 1, rhodamine B hydrazide was synthesized by following reported procedures¹⁻². To a 250 mL flask, rhodamine B (4.8 g, 10 mmol) was dissolved in 100 mL ethanol. Excess (18 mL) hydrazine hydrate was added drop-wise, and the mixture was refluxed overnight. The solution changed from dark pink to transparent orange. Then, the mixture was cooled and the solvent was removed by a rotary evaporator. The excess hydrazine hydrate was removed by washing with acid (1 M HCl). After that, 1 M NaOH was added slowly with stirring until the pH of the solution reached 8-9. The resulting precipitate was filtered, washed three times with pure water and then dried in the oven.

Yield= 87%. ¹H-NMR (CDCl₃, δ in ppm): 1.12-1.27 (t, 12H, NCH₂CH₃), 3.27-3.45 (t, 8H, NCH₂CH₃), 3.45-3.92 (d, 2H, NNH₂), 6.19-6.37 (s, 2H, ArH), 6.37-6.57 (t, 4H, ArH), 7.05-7.16 (t, 1H, ArH), 7.40-7.56 (t, 2H, ArH), 7.87-8.03 (q, 1H, ArH). Elemental analysis: calculated for C₂₈H₃₂N₄O₂ (MW: 456.59), C 73.66, H 7.06, N 12.27; found C 72.47, H 7.00, N 12.16.

Synthesis of the bis-rhodamine imine probe (BRI)

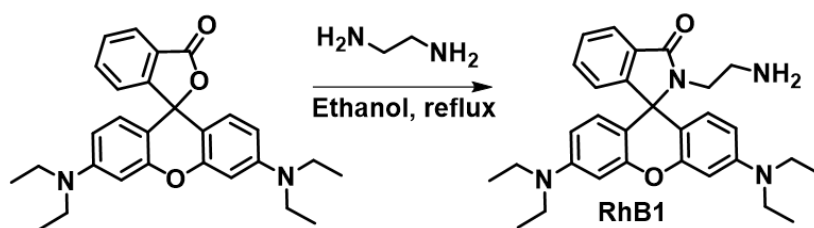


Rhodamine B hydrazide (1.5 g) was dissolved in 40 mL ethanol in flask. Then, glutaraldehyde (25% aqueous solution, 1.5 mL) was added. After being stirred well at room temperature for 6 h, the crude product precipitated out. The crude product was filtered, washed 3 times with ethanol, and then dried in the oven.

Yield= 55%. $^1\text{H-NMR}$ (CDCl_3 , δ in ppm): 1.04-1.09 (m, 24H, NCH_2CH_3), 1.19-1.26 (m, 2H, $-\text{CH}_2-$), 1.74-1.83 (d, 4H, $-\text{CH}_2-$), 3.17-3.39 (q, 16H, NCH_2CH_3), 6.12-6.25 (s, 4H, ArH), 6.32-6.42 (s, 4H, ArH), 6.42-6.54 (d, 4H, ArH), 6.98-7.09 (d, 2H, ArH), 7.35-7.48 (s, 4H, ArH), 7.52-7.63 (s, 2H, $-\text{N}=\text{CH}-$), 7.92-7.97 (d, 2H, ArH).

$^{13}\text{C-NMR}$ (CDCl_3 , δ in ppm): 13.0 (NCH_2CH_3), 31.8($-\text{CH}_2-$), 44.8 (NCH_2CH_3), 65.8 (NC-Ar), 98.0 (ArH), 106.4 (Ar), 108.5 (ArH), 123.5 (ArH), 127.7 (ArH), 133.2 (ArH), 149.1 (Ar), 152.9 ($-\text{N}=\text{CH}-$), 165.0 (CO).Elemental analysis: calculated for $\text{C}_{61}\text{H}_{68}\text{N}_8\text{O}_4$ (MW:977.27), C 74.97, H 7.01, N 11.47; found C 72.87, H 7.02, N 11.14.

Synthesis of RhB1



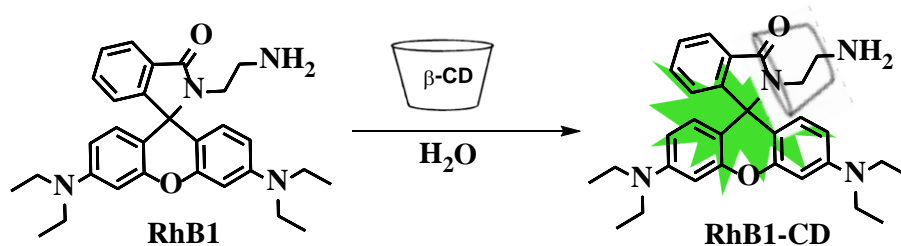
The compound RhB1 was synthesized by refluxing rhodamine B (4.8 g, 10 mmol) with excess ethylenediamine (5 mL) in ethanol until the solution lost its red color. After completion of the reaction, the solvent was removed by a rotary evaporator. The resultant solid was extracted with dichloromethane and washed with water several times. The organic layer was separated and dried over anhydrous MgSO_4 , and then the solvent was removed thoroughly. The resulting solid was washed with hot hexane (10 mL) and dried.

Finally, the crude solid was purified by column chromatography (eluent, EA:hexane = 1:3, $R_f = 0.45$).

Yield=80%. $^1\text{H-NMR}$ (400 MHz, CDCl_3) δ : 7.88–7.90 (d, 1H, ArH), 7.42–7.45 (m, 2H, ArH), 7.07–7.09 (d, 1H, ArH), 6.26–6.43 (m, 6H, ArH), 3.20–3.35 (q, 8H, NCH_2CH_3), 3.17–3.18 (t, 2H, $\text{NCH}_2\text{CH}_2\text{N}$), 2.41–2.43 (t, 2H, $\text{NCH}_2\text{CH}_2\text{N}$), 0.85–1.55 (t, 12H, NCH_2CH_3).

Molecular formula: $\text{C}_{30}\text{H}_{32}\text{N}_4\text{O}_2$ (484 g/mol).

Synthesis of RhB1-cyclodextrin inclusion complexes



The water-insoluble RhB1 synthesized above and water-soluble β -cyclodextrin (solubility in water 1.85 g/100 mL at 25°C) were mixed at a ratio of 1:2.5 (RhB1: β -CD) in water and vigorously stirred for 12 hrs. Stirring was continued until the solution become pink, and the mixture was allowed to stand for 2 hrs. The excess β -CD was removed by filtration, and the filtrate was concentrated to obtain pure RhB1-CD as a pink solid.

References

- (a) R. Balamurugan, C. C. Chien, B. C. Chen and J. H. Liu, *Tetrahedron*, 2012, In press.
(b) D. Wu, W. Huang, C. Y. Duan, Z. H. Lin, and Q. J. Meng, *J. Inorg. Chem.*, 2007, **46**, 1538.
(c) X. Zhang, Y. Shiraishi and T. Hirai, *Org. Lett.*, 2007, **9**, 5039.
- D. C. Choi, S. H. Kim, J. H. Lee, H. N. Cho, and S. K. Choi, *Macromolecules*, 1997, **30**, 176.

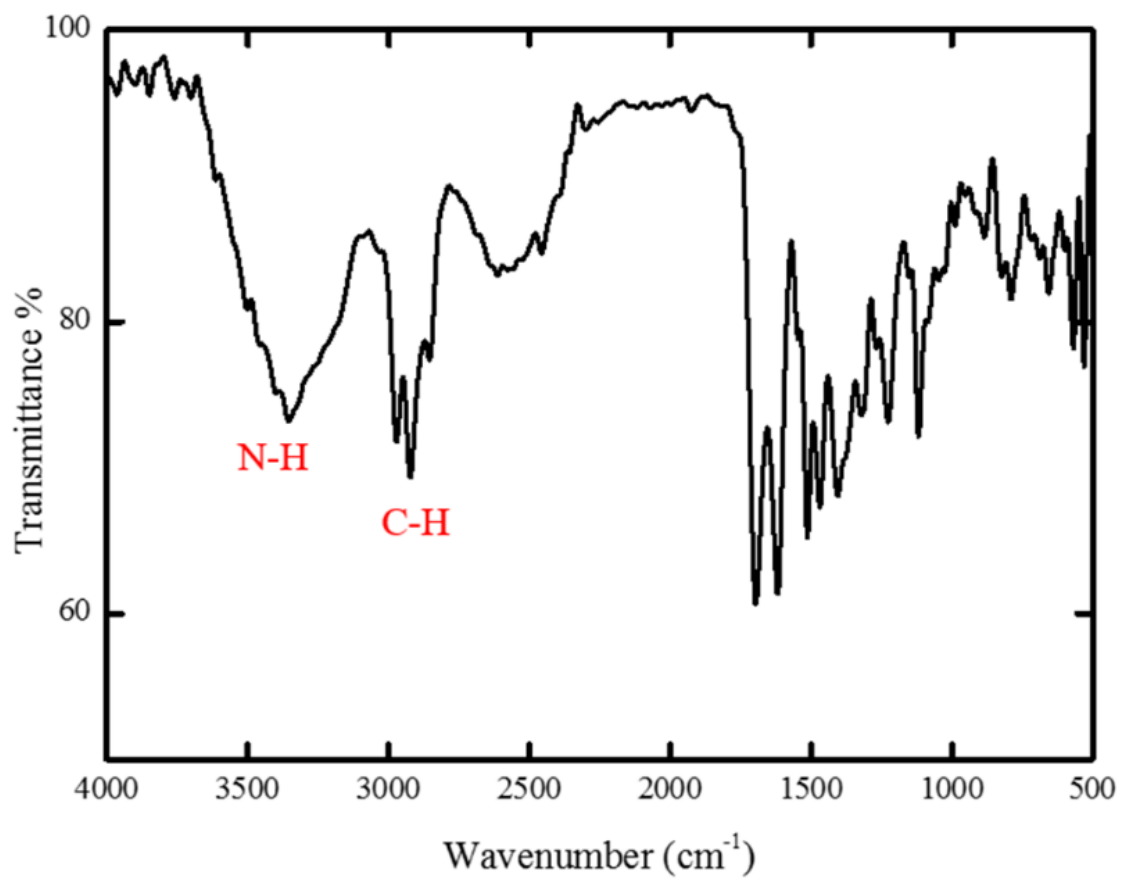


Fig. S1 Infrared spectrum of rhodamine B hydrazide

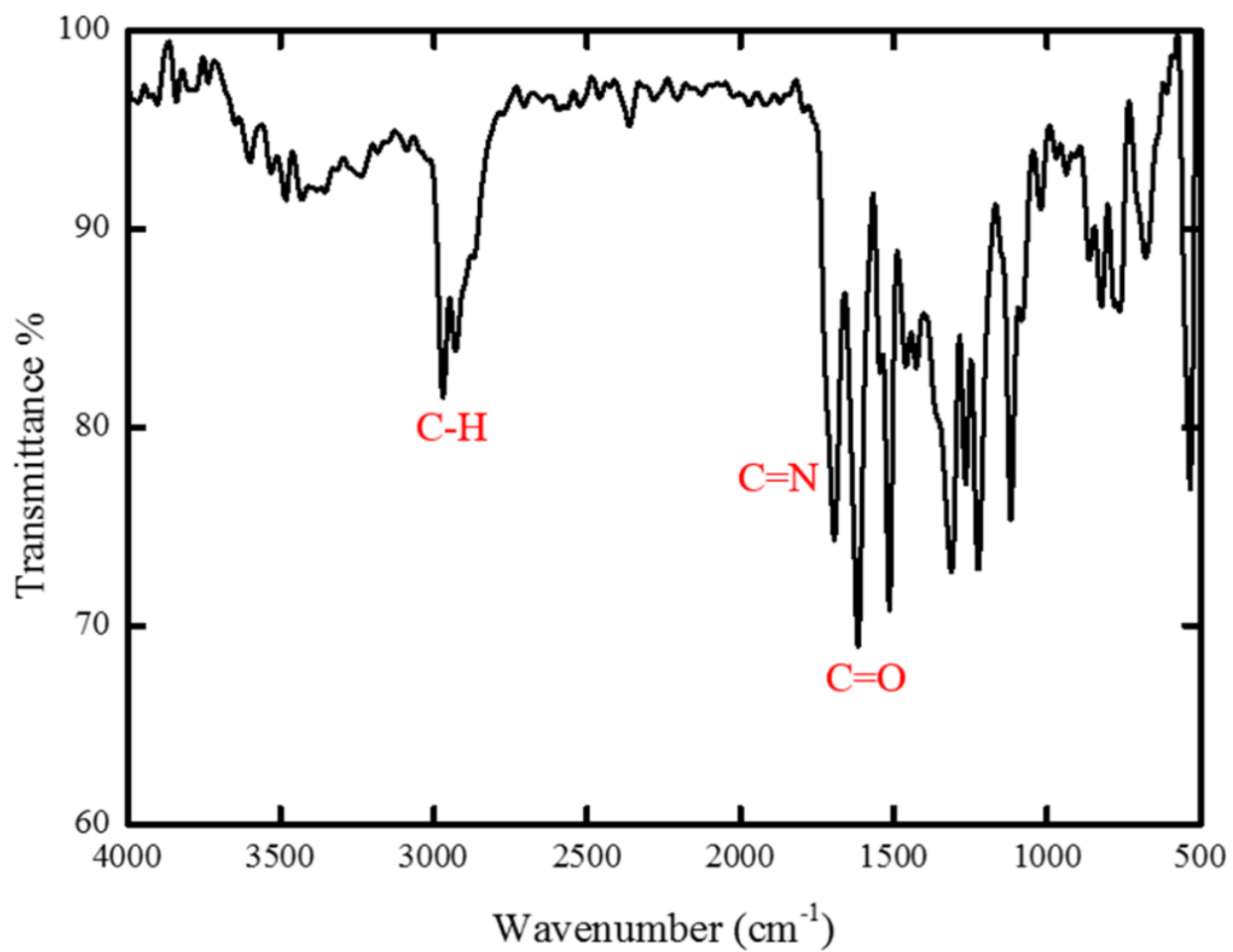


Fig. S2 Infrared spectrum of the **BRI** probe.

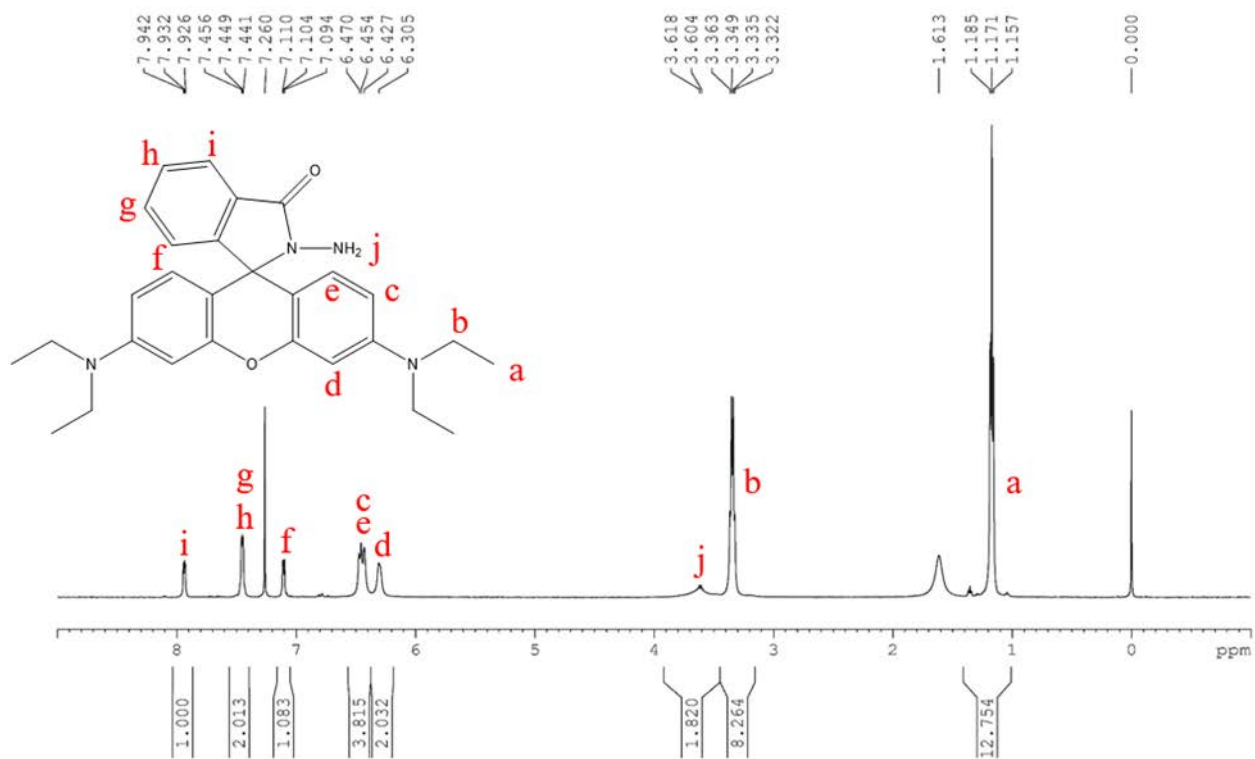


Fig. S3 ¹H-NMR spectrum of rhodamine B hydrazide in CDCl₃

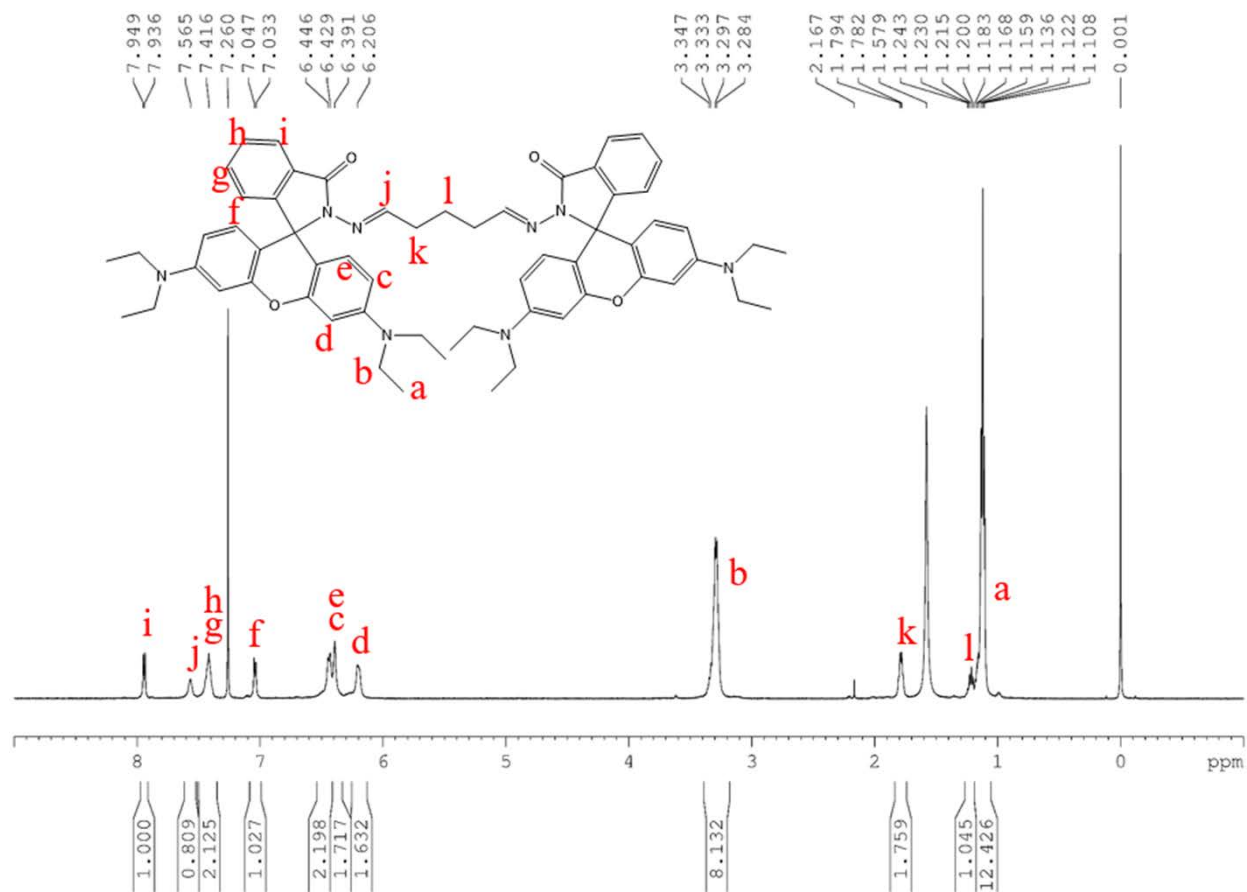


Fig. S4 ¹H-NMR spectrum of the probe **BRI** in CDCl₃.

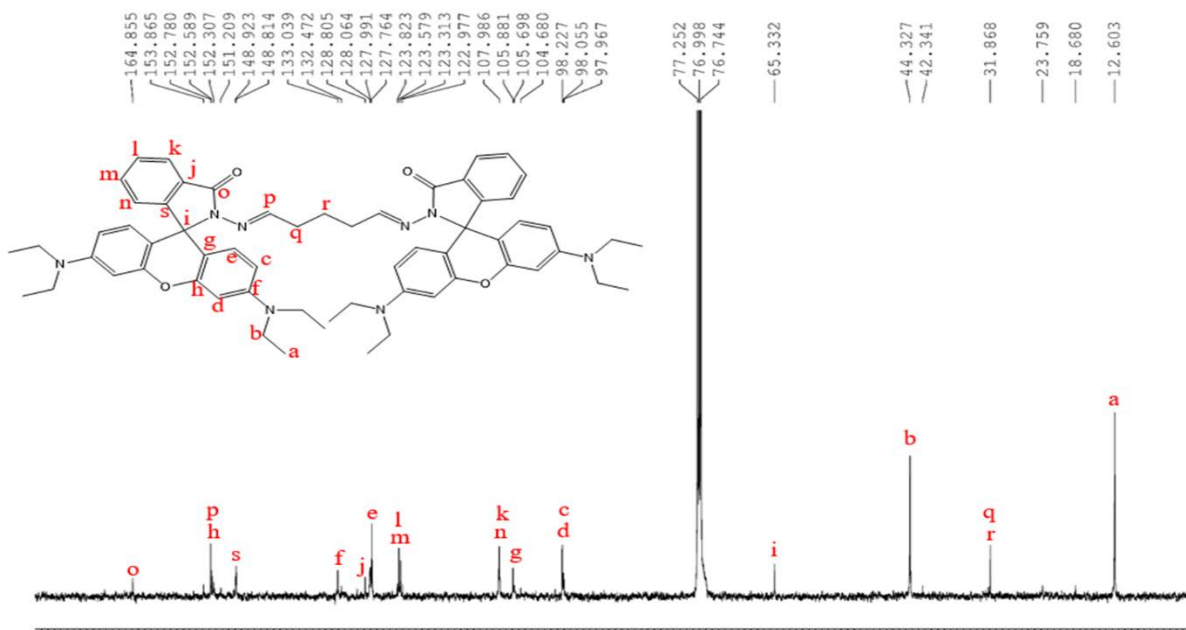


Fig. S5 ^{13}C -NMR spectrum of the probe **BRI** in CDCl_3

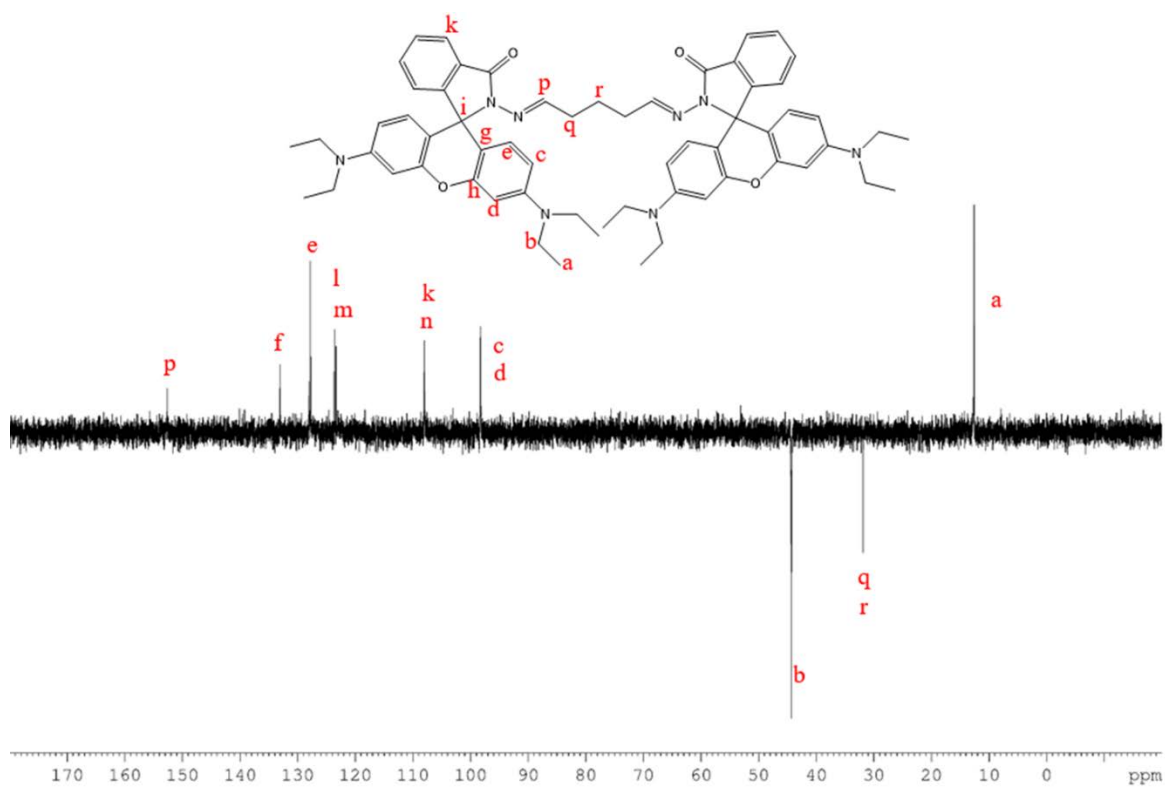


Fig. S6 DEPT135 ^{13}C -NMR spectrum of the probe **BRI** in CDCl_3

科技部台南貴重儀器使用中心
元素分析儀 elementar vario EL cube 服務報告書

使用者姓名: <u>陳宥任</u>	中心編號: <u>105-05-089</u>			
服務單位: <u>成大化工</u>	樣品名稱: <u>BRI</u>			
收件日期: <u>105</u> 年 <u>05</u> 月 <u>04</u> 日	完成日期: <u>105</u> 年 <u>05</u> 月 <u>09</u> 日			
分析結果:				
樣品重量: 1. <u>2.949</u> mg	2. <u>2.904</u> mg	3. <u>-----</u> mg		
實驗值:	N%	C%	H%	S%
1.	<u>11.14</u>	<u>72.87</u>	<u>7.02</u>	<u>-----</u>
2.	<u>11.12</u>	<u>72.78</u>	<u>7.03</u>	<u>-----</u>
3.	<u>-----</u>	<u>-----</u>	<u>-----</u>	<u>-----</u>
推測值:	<u>11.47</u>	<u>74.97</u>	<u>7.01</u>	<u>-----</u>
本日使用之標準樣品: A				
	(A) Acetanilide	(B) Nicotin Amide	(C) Sulfanilic Acid	
	N%	C%	H%	S%
理論值:	<u>10.36</u>	<u>71.09</u>	<u>6.71</u>	<u>-----</u>
測出值:	<u>10.39</u>	<u>71.11</u>	<u>6.76</u>	<u>-----</u>
建議:				
費用核算 : NCH: <u>1500</u>				
S: <u>-----</u>				
報告日期: <u>105</u> 年 <u>05</u> 月 <u>10</u> 日			預約序號: <u>050108</u>	

委託人非經本中心同意，不得將檢測結果用商業廣告之標示、法律訴訟之證據等其他用途，違者本中心將依法追訴。

技術員簽章：



Fig. S7 Elemental analysis of BRI

[Elemental Composition] Page: 1
 Data : 10505132 Date : 21-Jun-2016 11:47
 Sample: BRI
 Note : NBA
 Inlet : Direct Ion Mode : FAB+
 RT : 0.30 min Scan#: 8
 Elements : C 65/0, H 69/0, O 4/0, N 8/0
 Mass Tolerance : 1000ppm, 3mmu if m/z < 3, 5mmu if m/z > 5
 Unsaturation (U.S.) : -0.5 - 50.0

Observed m/z	Int%	Err[ppm / mmu]	U.S.	Composition
977.5439	100.0	-0.3 / -0.3	31.5	C 61 H 69 O 4 N 8

[Theoretical Ion Distribution] Page: 1
 Molecular Formula : C61 H69 O4 N8
 (m/z 977.5442, MW 978.2701, U.S. 31.5)
 Base Peak : 977.5442, Averaged MW : 978.2746(a), 978.2754(w)

m/z	INT.
977.5442	100.0000
978.5473	71.9726
979.5504	26.3194
980.5534	6.5178
981.5564	1.2284
982.5593	0.1877
983.5622	0.0242
984.5650	0.0027
985.5679	0.0003

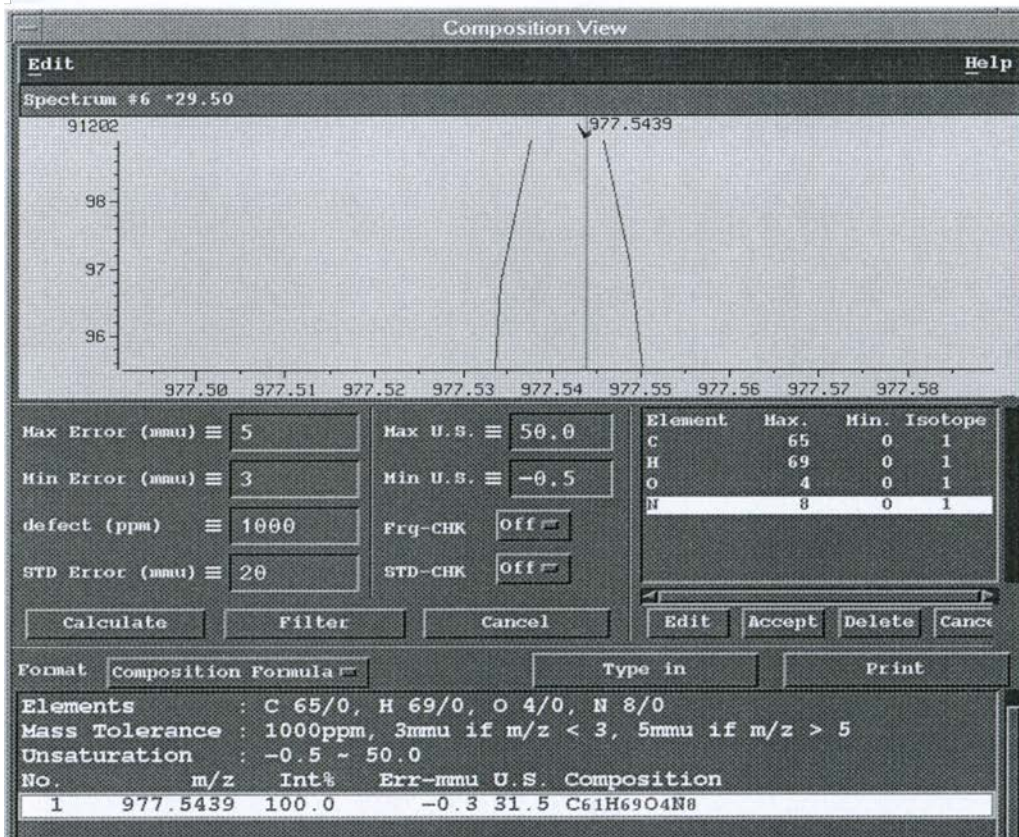


Fig. S8 Mass spectral analysis of BRI

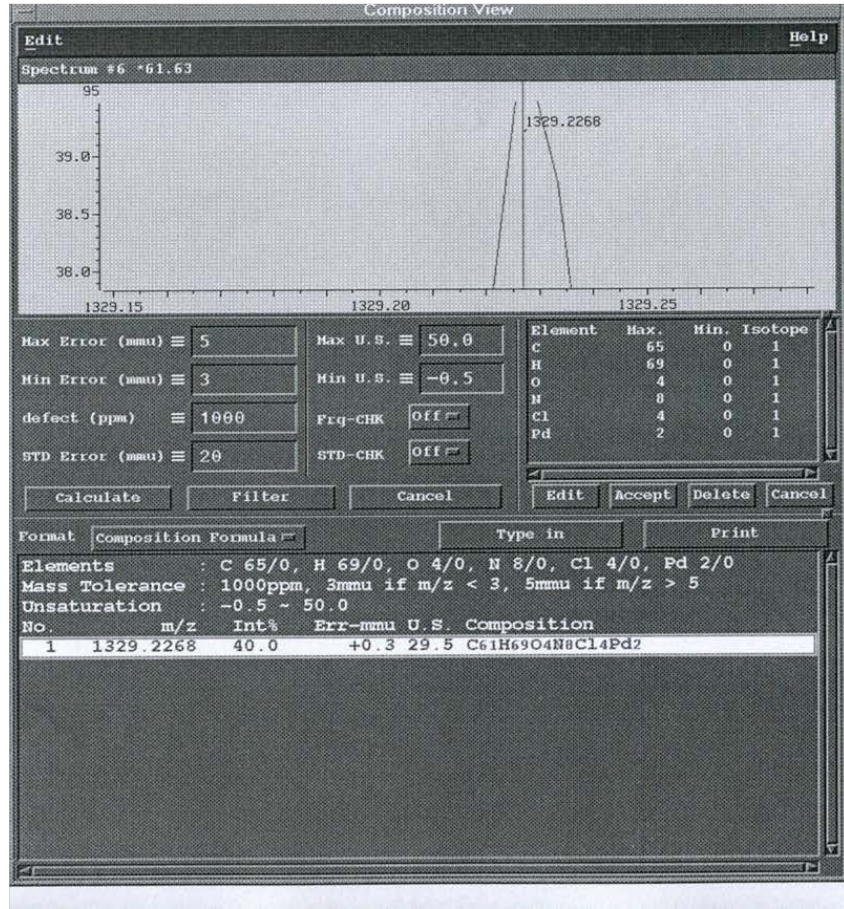
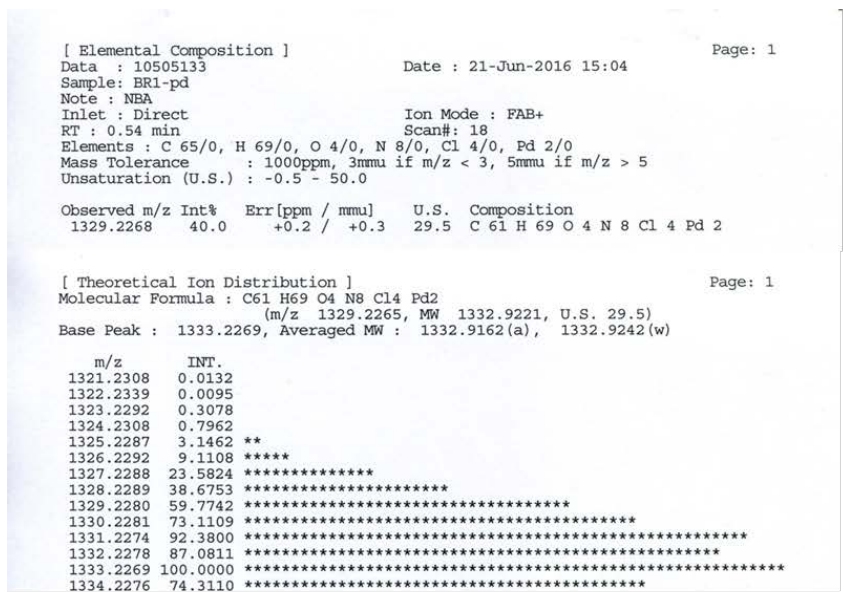


Fig. S9 Mass spectral analysis of Pd²⁺-BRI-Pd²⁺

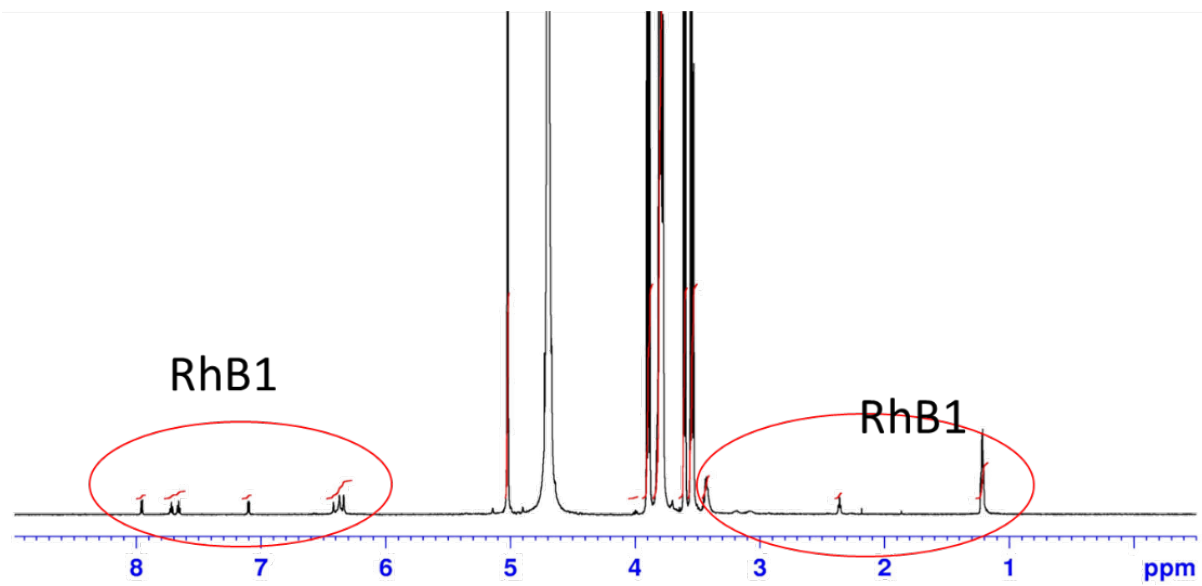


Fig. S10 $^1\text{H-NMR}$ spectrum of RhB1-CD in D_2O

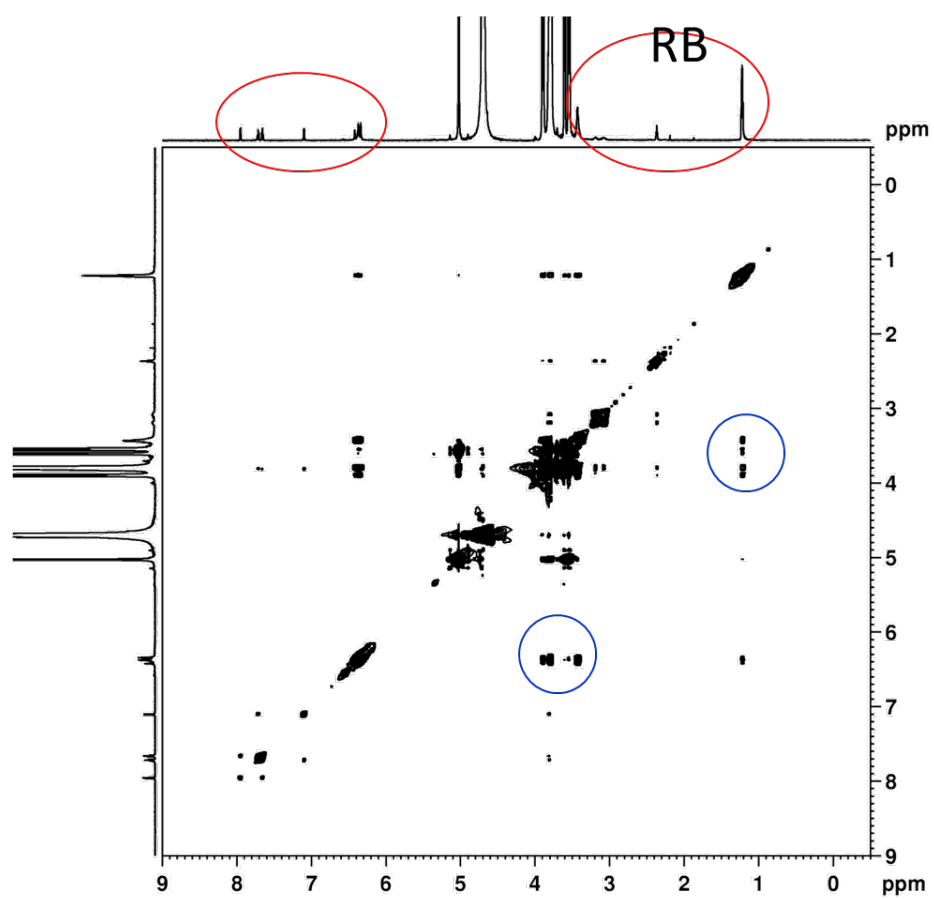


Fig. S11 2D- ^1H -NMR spectrum of RhB1-CD in D_2O

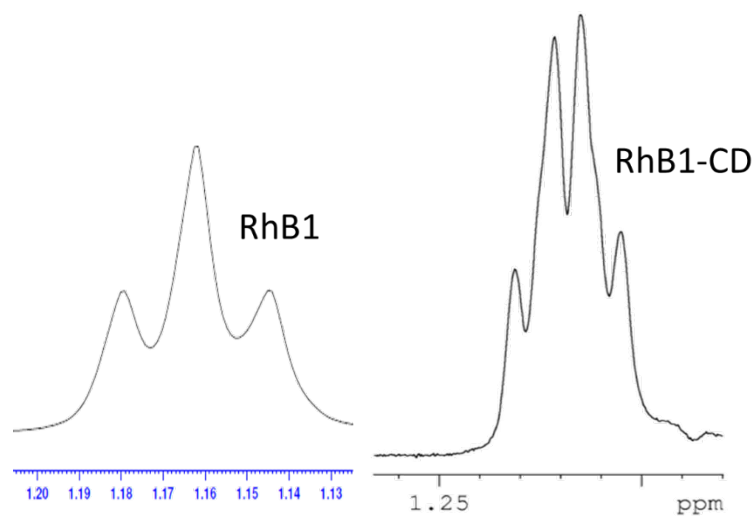


Fig. S12 Comparison of the ¹H-NMR signals of RhB1 and RhB1-CD between 1.1 and 1.2 ppm

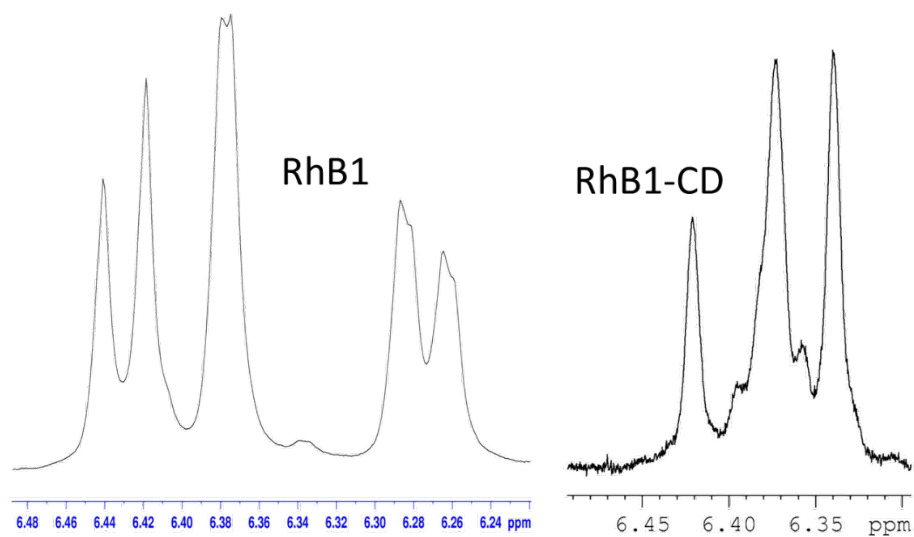


Fig. S13 Comparison of the ¹H-NMR signals of RhB1 and RhB1-CD between 6.2 and 6.5 ppm

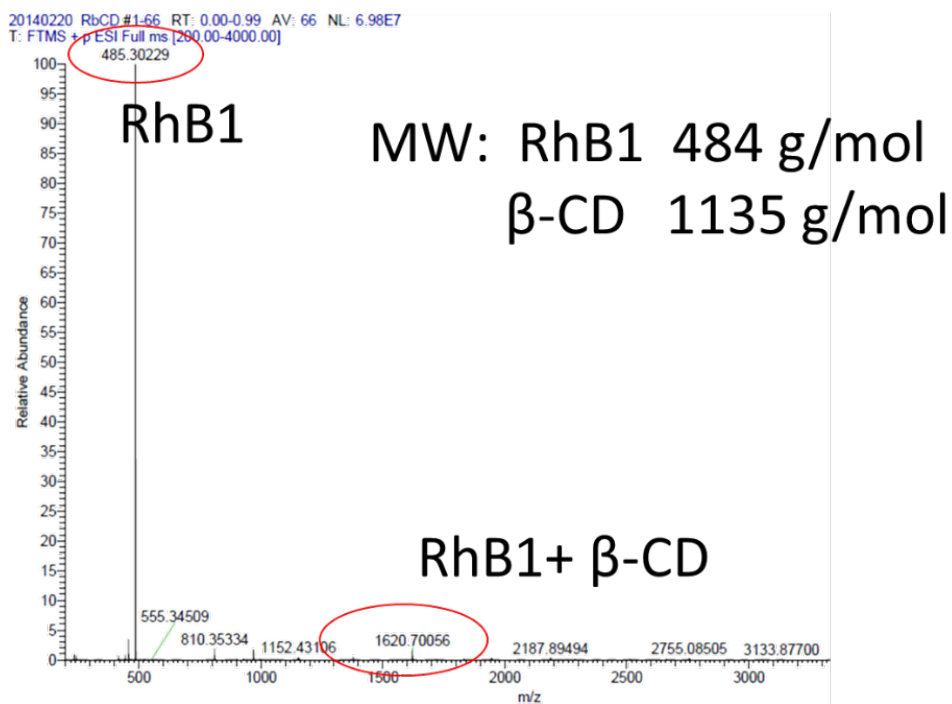


Fig. S14 Mass spectrum of RhB1-CD

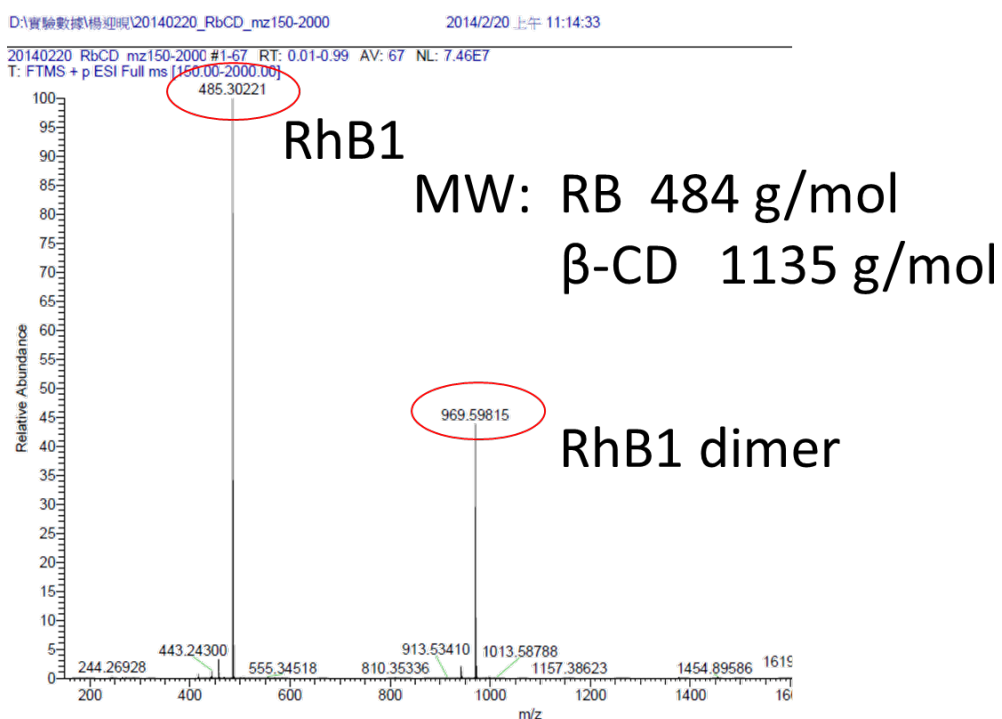


Fig. S15 Mass spectrum of RhB1-RhB1

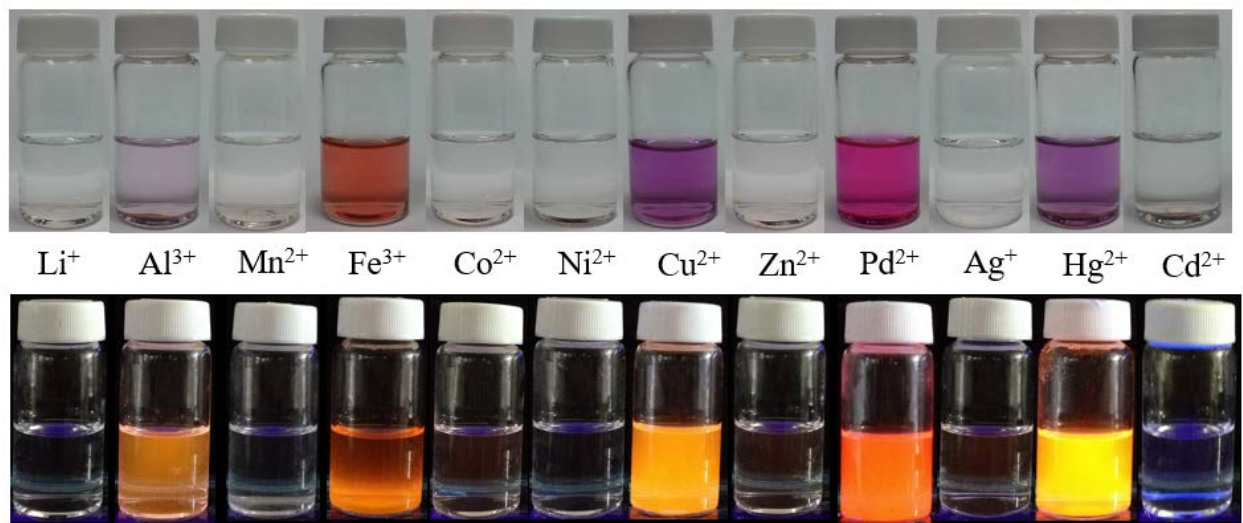


Fig. S16 Real images of BRI (10 μM) in CH₃CN:H₂O (3:2 v/v) in the presence of metal ions (1 mM, 100 equivalents) under visible light (top) and UV lamp (bottom). From left to right, the priority is Li⁺, Al³⁺, Mn²⁺, Fe³⁺, Co²⁺, Ni²⁺, Cu²⁺, Zn²⁺, Pd²⁺, Ag⁺, Hg²⁺, Cd²⁺.

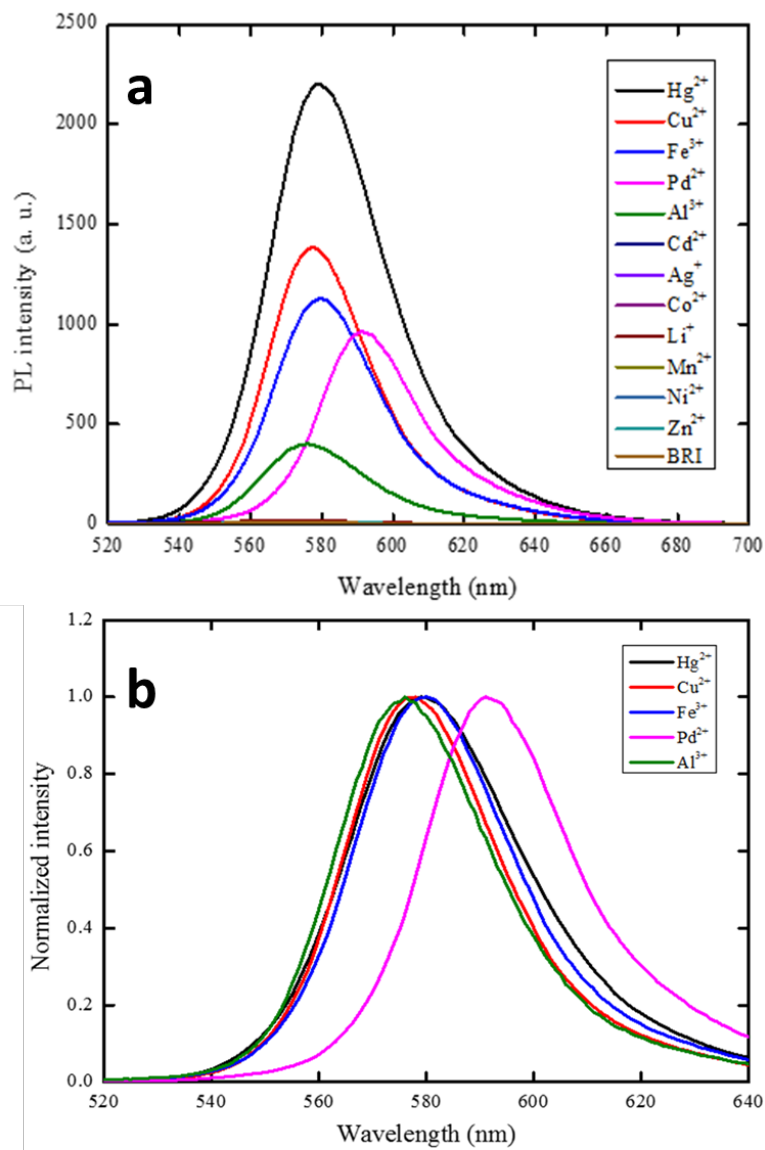


Fig. S17 (a) Fluorescence spectral changes of **BRI** (10 μ M) upon addition of 100 equivalents of metal ions (Hg^{2+} , Cu^{2+} , Fe^{3+} , Pd^{2+} , Al^{3+} , Cd^{2+} , Ag^{2+} , Co^{2+} , Li^{+} , Mn^{2+} , Ni^{2+} and Zn^{2+}). (b) Normalized fluorescence spectra of BRI (10 μ M) in $\text{CH}_3\text{CN}:\text{H}_2\text{O}$ (3:2 v/v) in the presence of metal ions (1 mM, 100 equivalents); $\lambda_{\text{ex}}=510$ nm.

Recognition of metal ions as a function of time

Before recording the spectra of the complexes, the samples were incubated for 30 min after the addition of each metal solution, and then the spectra were recorded. The time study revealed that **BRI** (λ_{\max}) recognition of metal is completed within 20-30 min of the addition of the metal ion, as shown below (time taken to measure each spectrum was not accounted).

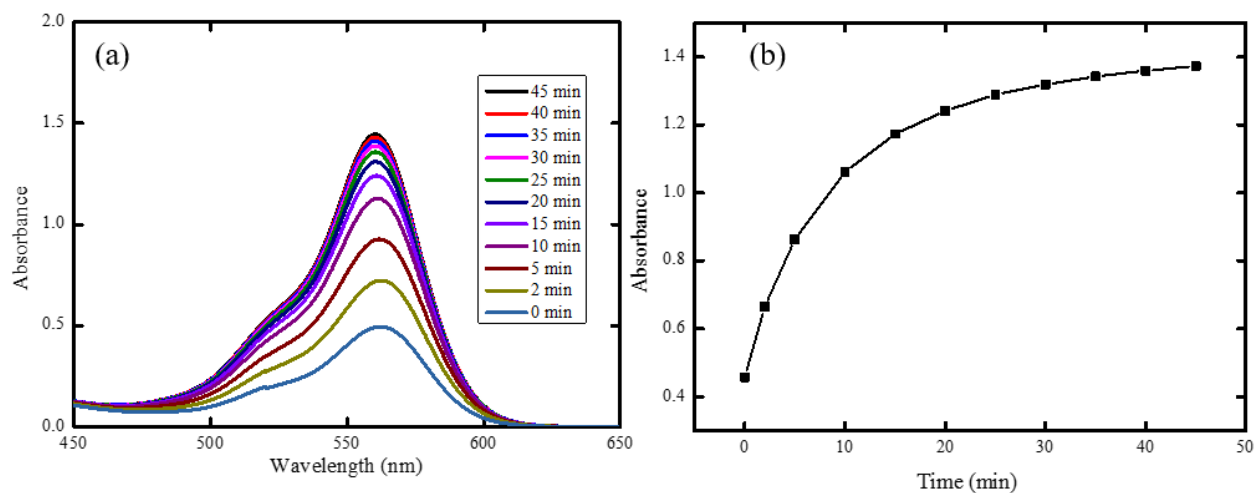


Fig. S18 (a) Time-dependent UV-vis spectra of **BRI** (10 μM) with 100 equivalents of Pd^{2+} in $\text{CH}_3\text{CN}:\text{H}_2\text{O}$ (3:2 v/v). (b) Plot of the absorbance of **BRI**/ Pd^{2+} at 555 nm as a function of time.

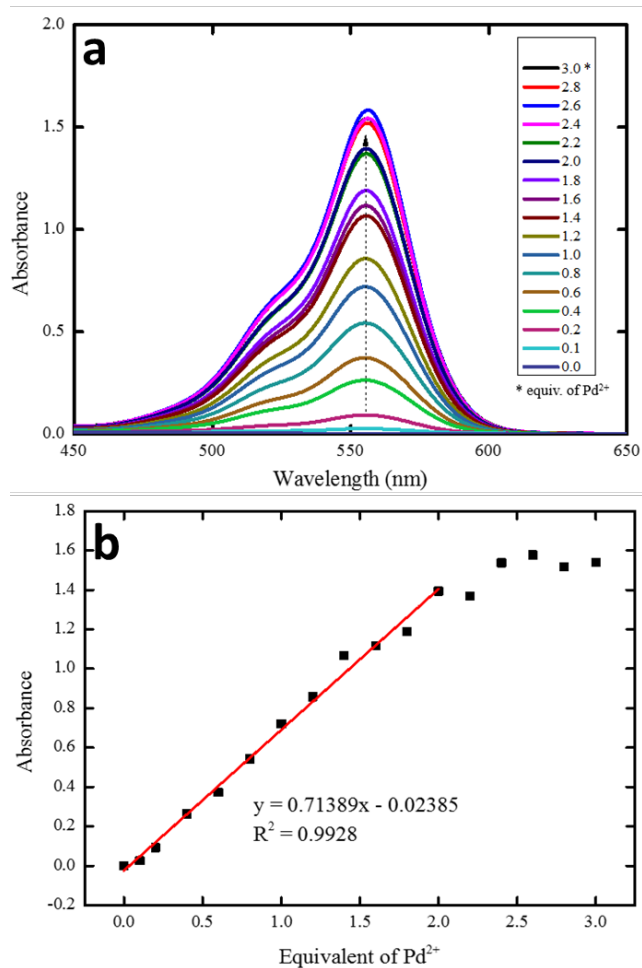


Fig. S19 (a) UV-vis spectra of BRI (10 μM) in CH₃CN:H₂O (3:2 v/v) solution containing various amounts of Pd²⁺ ions (0.0-3.0 equivalents), λ_{max}=555 nm. (b) Plot of the absorbance of BRI versus the amounts of Pd²⁺ (0.0-3.0 equiv.) at λ=555 nm.

Job Plot

The results from the Job plot showed that the value of $x=0.64$, indicating that the most preferred coordinated structure formed at this point. Given that the relationship between $[\mathbf{BRI}] + [\text{Pd}^{2+}] = 1$ and that $[\text{Pd}^{2+}]/[\mathbf{BRI}] = 0.64$, it could be calculated that $[\text{Pd}^{2+}] = 0.64$, $[\mathbf{BRI}] = 0.36$, indicating that one **BRI** molecule could coordinate with approximately 2 Pd^{2+} ions.

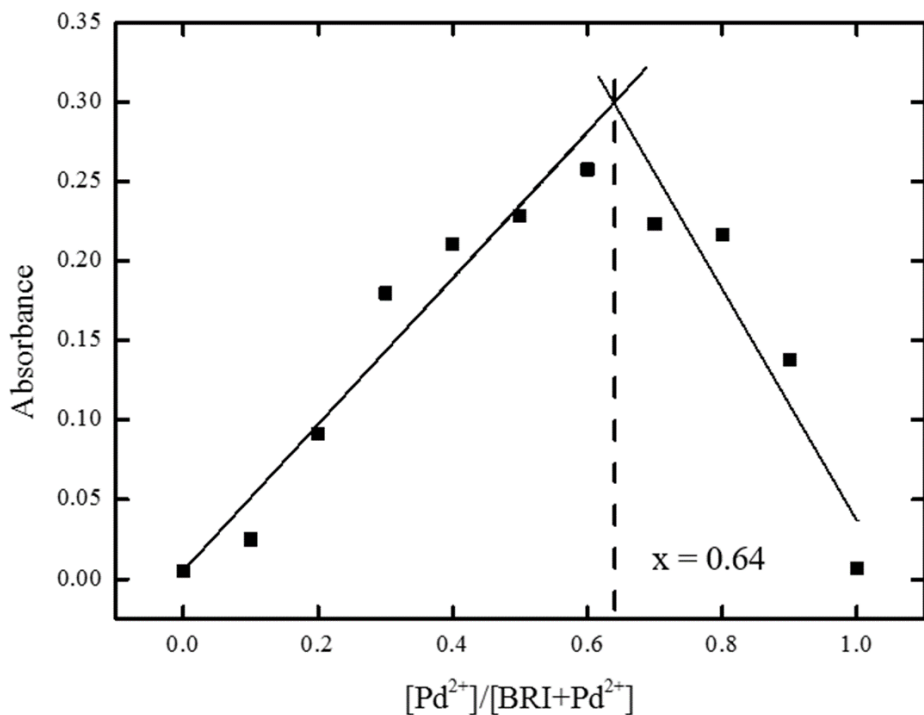


Fig. S20 The Job plot for **BRI-Pd²⁺** showed 1:2 complexes ($\text{BRI} : \text{Pd}^{2+} = 1 : 1.78$)

Hill's plot

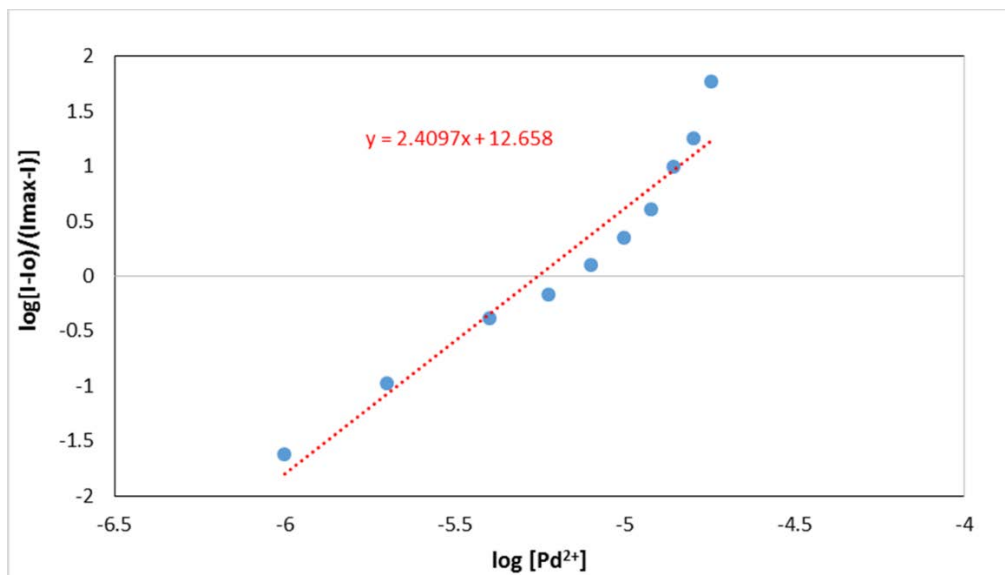


Fig. S21 Hill plot of the fluorescent probe BRI with Pd^{2+}

Binding constant

The binding constant of BRI with Pd^{2+} was determined using the Benesi-Hildebrand equation as follows:

$$\log\left(\frac{I-I_0}{I_{\text{MAX}}-I}\right) = n \times \log[M] - \log K_d$$

where I_0 : blank sample fluorescence intensity; I : complex sample fluorescence intensity; I_{MAX} : maximum fluorescence intensity of the complex; $[M]$: Pd^{2+} concentration; K_d : dissociation constant; K_a : association constant = $1/K_d$

From the plot, it was observed that $Y=2.4097x + 12.658$.

Therefore, $-\log K_d=12.658$, so $K_d=2.19 \times 10^{-13}$.

Therefore, the binding constant $K_a=1/K_d= 1/(2.19 \times 10^{-13})= 4.57 \times 10^{12}$.

Effect of pH

Fig. S5 shows the effect of pH on the absorption intensity of **BRI** (5 μM) in $\text{CH}_3\text{CN}:\text{H}_2\text{O}$ (1:1). The pH of the solution was adjusted by HCl (1 M) or NaOH (1 M) ($\lambda_{\text{ex}}=510 \text{ nm}$). The results indicated that **BRI** can work well near a neutral pH range (6-8) for Pd^{2+} detection.

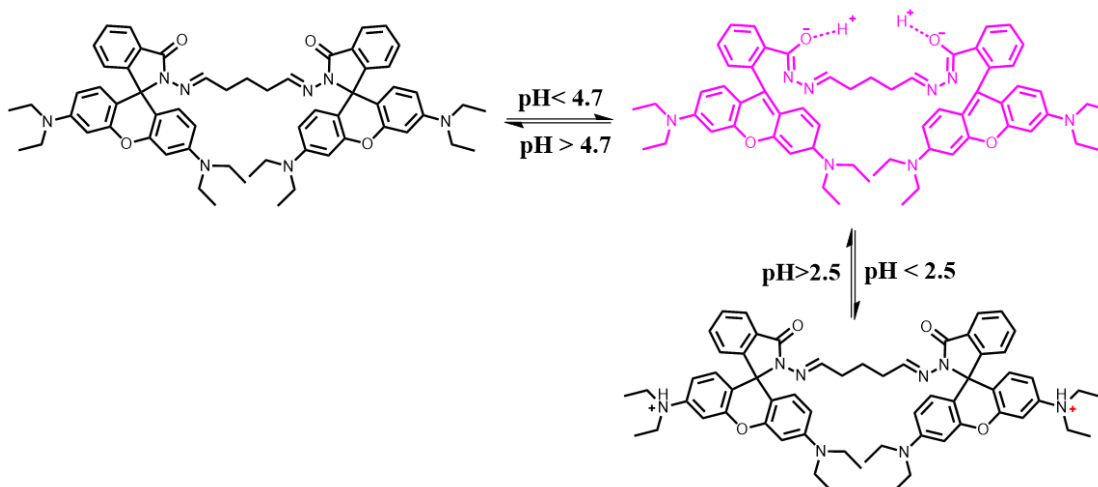
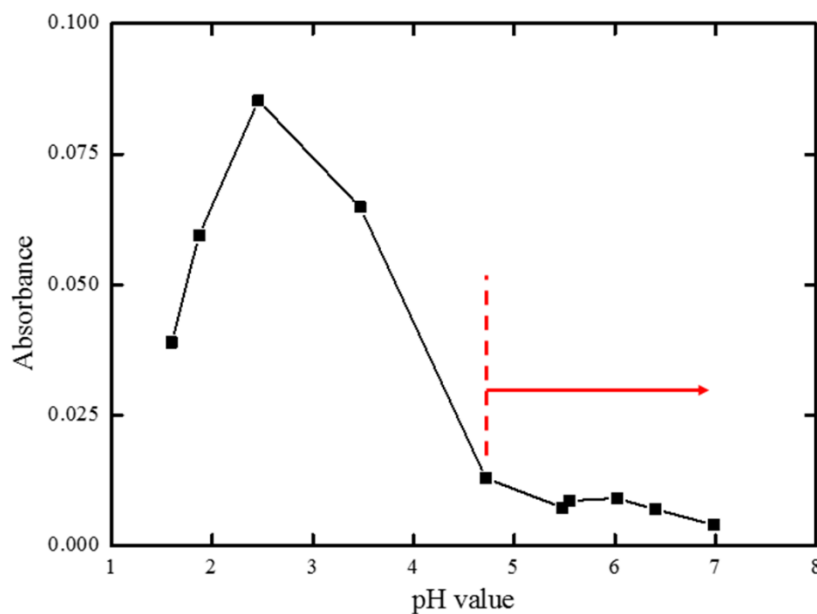


Fig. S22 (a) Effect of pH on absorbance of **BRI** (10 μM) at 555 nm in $\text{CH}_3\text{CN}:\text{H}_2\text{O}$ (3:2 v/v), where pH was adjusted using HCl (0.01 M). (b) Effect of pH on the structure of **BRI**

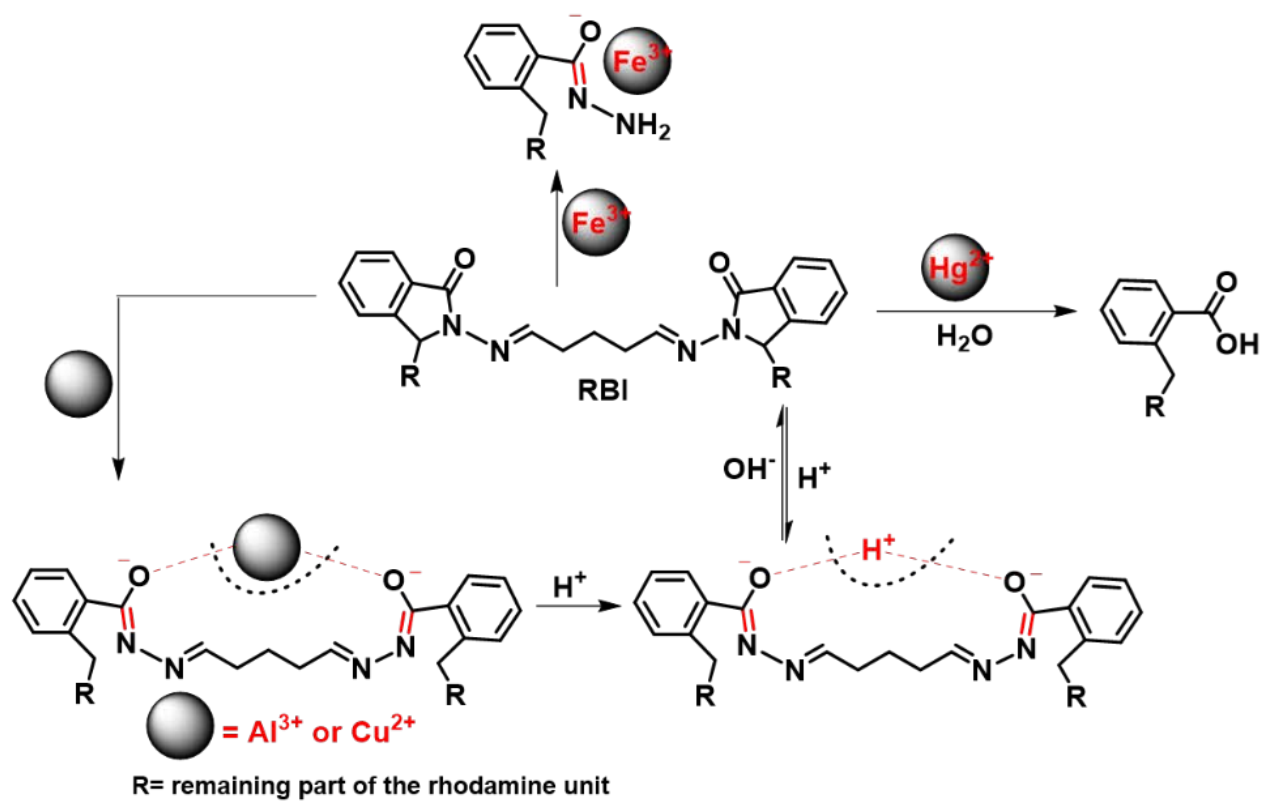


Fig. S23 Interaction of various metal ions with **RBI**

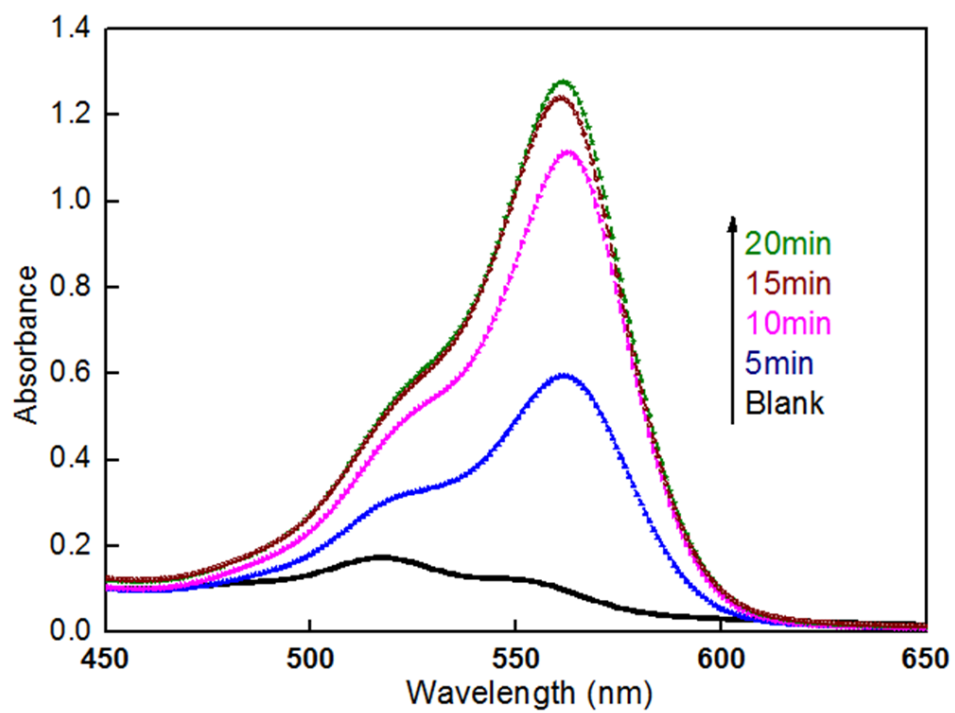


Fig. S24 Time-dependent UV-vis spectra of **RhB1-CD** (1 mM) with one hundred equivalents of Pd²⁺ in H₂O.

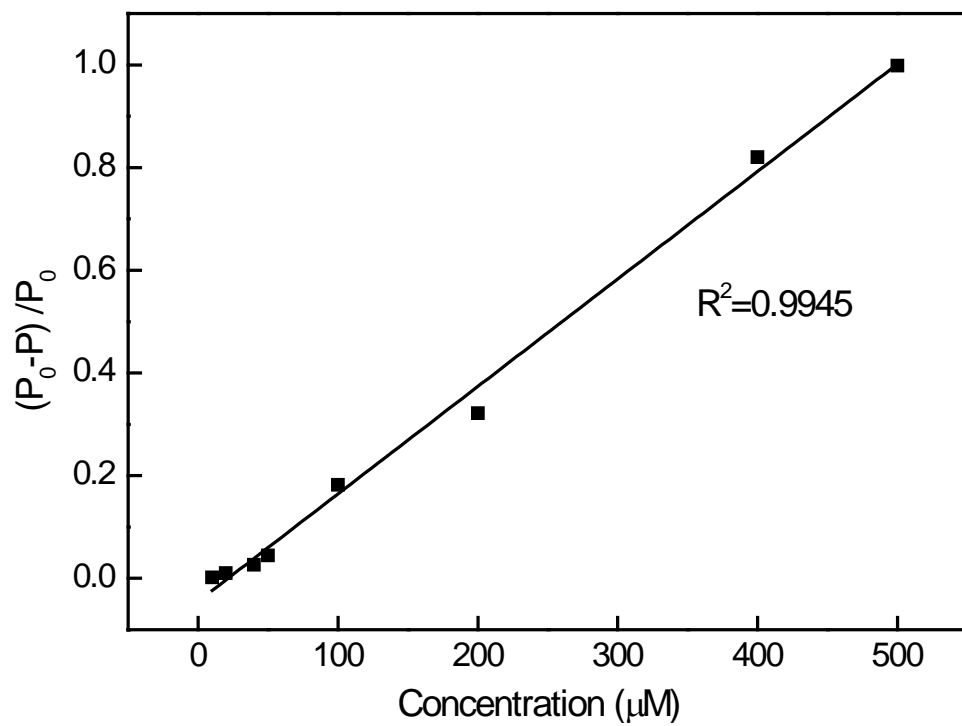


Fig. S25 Dependence of quenching ratio of RhB1-CD on Pd^{2+} concentration

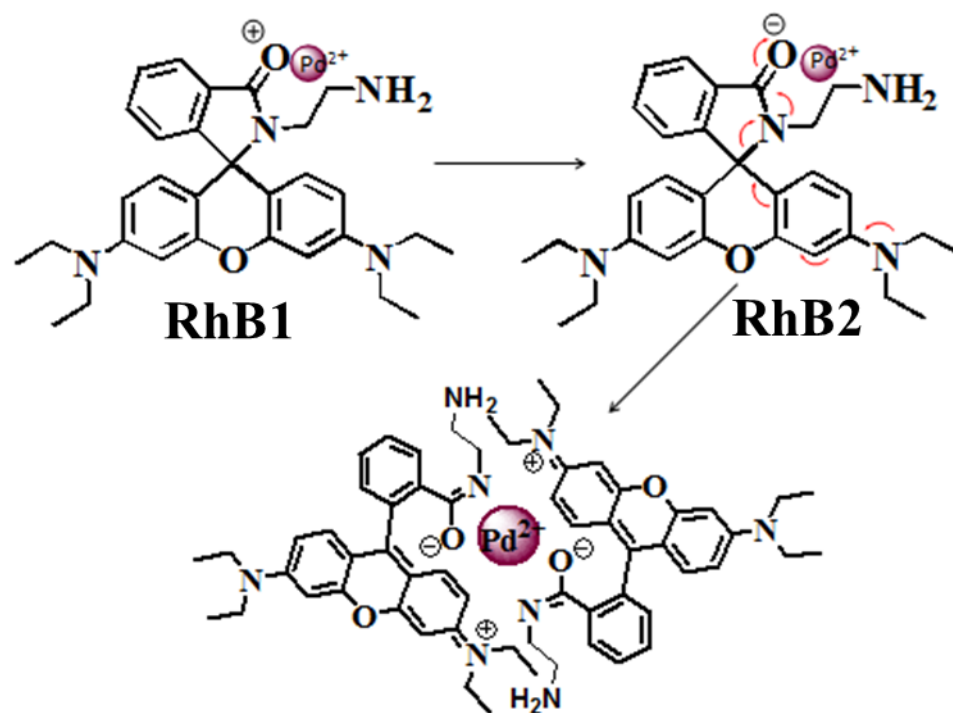


Fig. S26. Binding mechanism of RhB1 with Pd^{2+} in EtOH:H₂O (1:1)

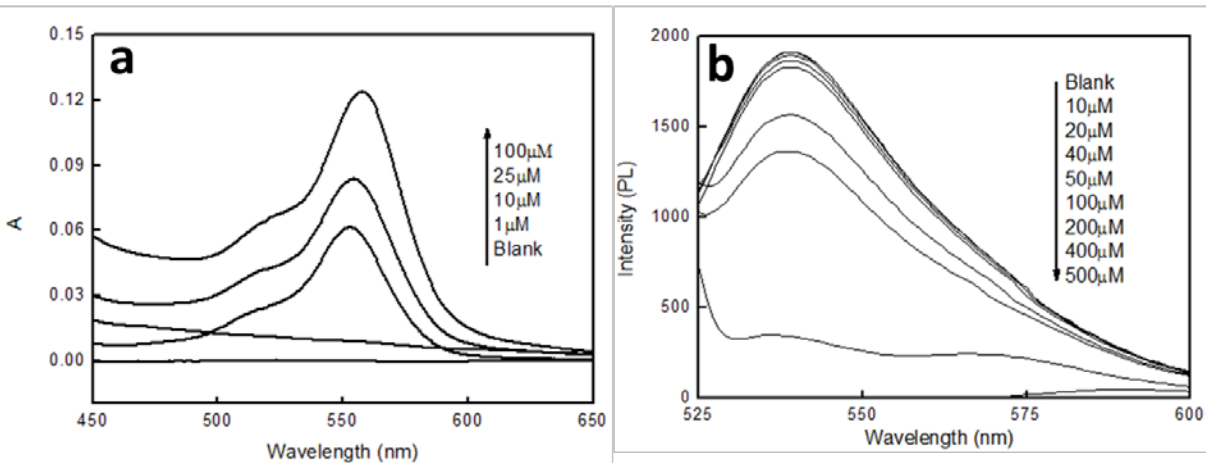


Fig. S27 Dependence of (a) UV-vis and (b) PL spectra of RhB1-CD on Pd²⁺ concentration in H₂O at pH 7.0.

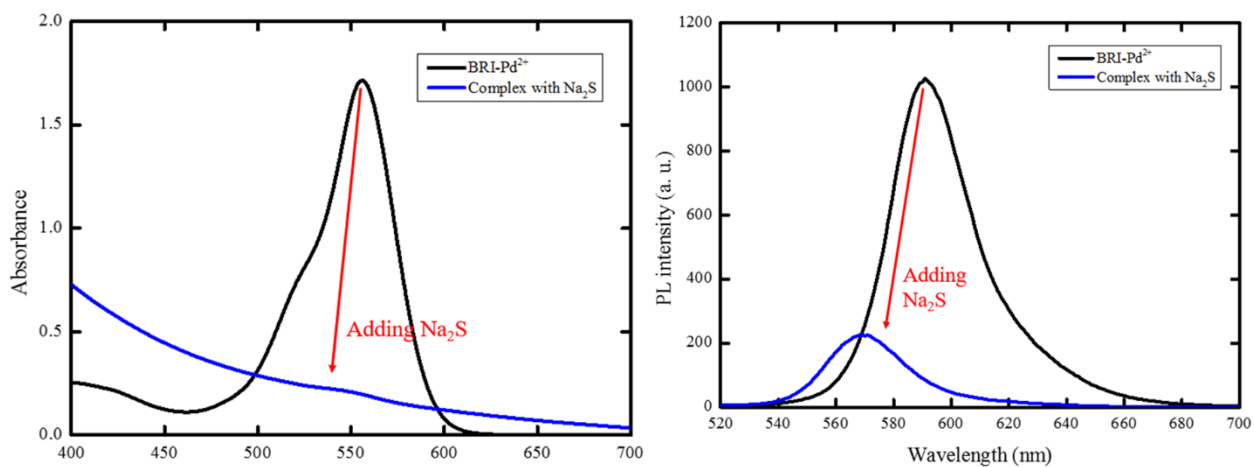


Fig. S28 Titration of BRI-Pd²⁺ complexes with Na₂S under (a) UV-vis and (b) fluorescence spectroscopy

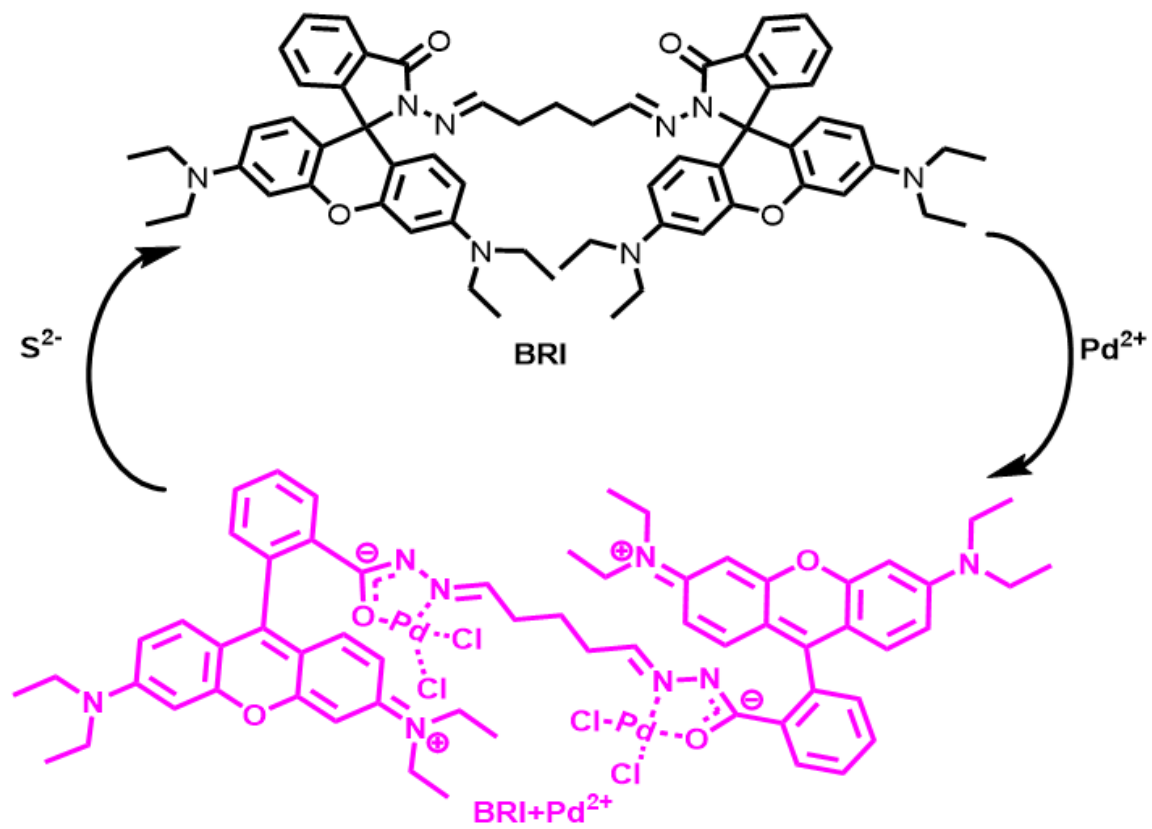


Fig. S29 Reversible process of BRI in the presence of Na_2S

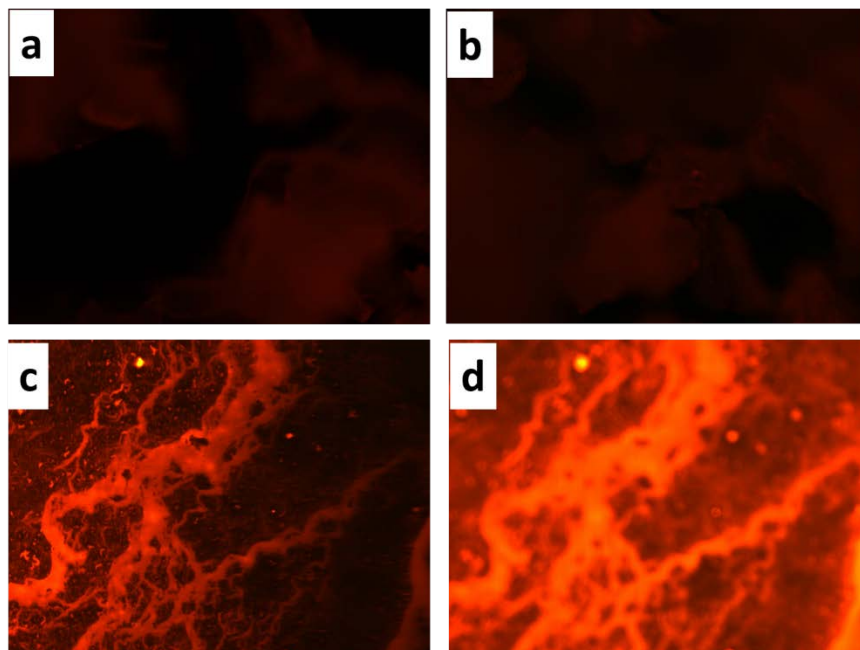


Fig. S30. Fluorescence images of BRI (a and b) and BRI-Pd²⁺ (c and d) under confocal laser scanning microscopy respectively.